HHS Public Access

Author manuscript

J Orthop Res. Author manuscript; available in PMC 2020 February 01.

Published in final edited form as:

J Orthop Res. 2019 February ; 37(2): 490–502. doi:10.1002/jor.24179.

Full-Thickness Rotator Cuff Tear In Rat Results In Distinct Temporal Expression Of Multiple Proteases In Tendon, Muscle, And Cartilage

Elda A. Treviño[1], **Jennifer McFaline-Figueroa**[1], **Robert E. Guldberg**[2,3], **Manu O. Platt**[1,2], **Johnna S. Temenoff**[1,2]

[1]Wallace H. Coulter Department of Biomedical Engineering [2]Parker H. Petit Institute for Bioengineering and Bioscience [3]George W. Woodruff School of Mechanical Engineering

Abstract

The etiology of joint tissue degeneration following rotator cuff tear remains unclear. Thus, the purpose of this study was to understand the timeline of protease activity in the soft tissues of the shoulder (tendon, muscle, and cartilage) that may lead to down-stream degeneration following rotator cuff tear. A well-established rat model involving suprascapular nerve denervation and supraspinatus/infraspinatus tendon transection was employed. Histological staining and/or micro-computed tomography (μCT) were used to observe structural damage in the supraspinatus tendon and muscle, humeral head cartilage, and subchondral bone. Multiplex gelatin zymography was utilized to assess protease activity in the supraspinatus tendon and muscle, and humeral head cartilage. Zymography analysis demonstrated that cathepsins were upregulated in the first week in all tissues, while MMP-2 maintained prolonged activity in supraspinatus tendon between 1 and 3 weeks and increased only at 3 weeks in supraspinatus muscle. In supraspinatus tendon, increased cathepsin L and MMP-2 activity in the first week was concurrent with matrix disorganization and infiltration of inflammatory cells. In contrast, significant upregulation of cathepsin L and K activity in supraspinatus muscle and humeral head cartilage did not correspond to any visible tissue damage at one week. However, focal defects developed in half of all animals' humeral head cartilage by 12 weeks (volume: 0.12 ±0.09 mm^3). This work provides a more comprehensive understanding of biochemical changes to joint tissue over time following rotator cuff tear. Overall, this provides insight into potential therapeutic targets and will better inform ideal intervention times and treatments for each tissue.

Keywords

Rotator cuff tendon; rotator cuff muscle; cartilage; cathepsin; matrix metalloproteinase

Correspondence to: Johnna S. Temenoff, Wallace H. Coulter Department of Biomedical Engineering, 315 Ferst Dr. Atlanta, GA 30318, johnna.temenoff@bme.gatech.edu, Tel: 1-404-385-5026, Fax: 1-404-894-4243.

AUTHOR CONTRIBUTIONS STATEMENT

Treviño and Temenoff designed the study, analyzed the data, and prepared the manuscript. Treviño and McFaline-Figueroa collected and analyzed the data. Guldberg and Platt helped analyze the data and prepare the manuscript. All authors have read and approved the final submitted manuscript.

INTRODUCTION

Rotator cuff tears, including partial and full-thickness tears of the supra- and infraspinatus tendons, are among the most common shoulder injuries and result in over 75,000 surgical repairs annually[1]. Following rotator cuff tear, several tissues are negatively affected including the tendon, its respective muscle, and articular cartilage in the shoulder joint. Such damage includes tendon disorganization with decreased collagen content[2], muscle atrophy, and fibrous tissue and fatty deposits within the muscle[3]. Additionally, the force balance between tendons of the rotator cuff is disrupted, which may lead to the development of osteoarthritic changes in the articular cartilage including loss of glycosaminoglycan (GAG) content, increased surface roughness, and loss of cartilage tissue[4,5].

While damage to joint tissue following rotator cuff tear is well documented, the exact biochemical processes responsible for extracellular matrix (ECM) turnover that contribute to this damage remain unknown. In joint tissues, both ECM components and the proteases that degrade them are secreted for the purposes of tissue remodeling[6]. For example, tenocytes have been shown to alter the rate of collagen synthesis[7] as well as protease secretion[8] in response to changes in mechanical loading. Furthermore, an acute injury such as rotator cuff tendon tear could incite an inflammatory response, whereby inflammatory cells such as neutrophils and macrophages would be recruited to the area. It is well known that inflammatory cells have the capacity to secrete proteases[9,10] that may further contribute to the net shift towards ECM degeneration. Thus, an imbalance between anabolic and catabolic factors through the increased presence of active proteases could be responsible for the decrease in ECM components, such as collagen and elastin[11,12], observed following rotator cuff tendon tear.

Cathepsins, papain-family cysteine proteases known to be some of the most powerful elastases and collagenases, are often associated with ECM remodeling and therefore warrant investigation in rotator cuff tear pathology[13]. Cathepsin K, canonically associated with osteoclasts and bone remodeling, has been previously observed in osteoporosis and osteoarthritis[14,15]. In particular, prior work has identified a positive correlation between amount of cathepsin K present and osteoarthritis severity in mice[16] and cathepsin L has been shown to be upregulated in instances of muscle atrophy in both rats and mice[17,18]. Additionally, our previous work investigating tendinopathy[19,20] has demonstrated upregulated cathepsin activity in the tendon at 4 and 8 weeks of overuse in a rat model.

Furthermore, matrix metalloproteinases (MMPs), zinc-dependent endopeptidases that play a role in ECM remodeling, have been previously implicated in tendon degeneration, muscle atrophy, and osteoarthritis development. Specifically, MMP-1 activity has been shown to be significantly greater in human supraspinatus tendon following rupture[21] and MMP-1 and -3 have been shown to be upregulated within synovial fluid following rotator cuff tendon tear in humans[22]. Additionally, MMP-2, -9, and -13 have been shown to be more active in osteoarthritic cartilage compared to healthy cartilage in both humans and rats[23,24], while increases in MMP-2 and -9 activity positively correlated with the occurrence of muscle atrophy in rats[18,25].

Both the cathepsin and MMP families contain potent collagenases and elastases, and thus are often seen in the same degenerative injury. For example, cathepsin L and MMP-2 have been observed to be upregulated in instances of muscle atrophy[18,25]. Interestingly, while both families of proteases can cleave collagen, they do so at different locations within the molecule and at different catalytic rates[17], and thus may act synergistically to enhance ECM degradation. Furthermore, cathepsins have the ability to cleave and activate pro-MMPs[26], which suggests they can work sequentially to digest collagen and promote tissue degradation[17]. Due to their shared substrates and cross-activation, it is important to investigate both families of enzymes individually and in connection to one another to better understand how proteases play a role in tissue degeneration after rotator cuff tear.

Thus, using early, middle, and late time points (1, 3, and 12 weeks respectively), the objective of this study was to characterize the protease activity profile over time in joint tissue following acute, full-thickness rotator cuff tear, and to relate these results to the timing of observed tissue structural damage, as monitored by histology or microcomputed tomography (μCT) imaging. To our knowledge, no work has investigated both families of proteases within all three soft tissues of the joint after full-thickness rotator cuff tears. We hypothesize that acute, full-thickness rotator cuff tear will result in significantly more protease activity (cathepsins and MMPs) early after injury in supraspinatus tendon (1 week), with delayed responses from cartilage and supraspinatus muscle (3-12 weeks after injury). Additionally, we hypothesize that protease upregulation timing will coincide with manifestation of visible tissue damage (as assessed by histology and/or μCT imaging) in each tissue. A summary of outcome measures for each tissue over time can be found in Table 1.

METHODS

Surgical Procedure and Outcome Measure Time Points

Rotator cuff injury was induced using a method previously established[27,28]. This animal model was chosen as muscle degeneration, an outcome we aim to characterize in this study, does not occur to a large degree in other models, such as tendon transection only, in rats[29]. Male Sprague-Dawley rats (N=30 total, 250-300 g initial weight and 8-10 weeks old) were used in accordance with protocols approved by the Georgia Institute of Technology Institutional Animal Care and Use Committee (Protocol #A15050). To induce injury, on the left side of the animal, a 5 mm portion of the suprascapular nerve was resected and both the supraspinatus and infraspinatus tendons were transected at the insertion into the humeral head. The wound was closed using Vicryl 4-0 absorbable sutures (Ethicon) and wound clips. The right forelimb of each animal served as an internal, uninjured contralateral control. Because rats are quadrupeds and do not have a dominant forelimb for daily activities, we did not deem it necessary to randomize for this study.

Time points for this study were chosen based on previous data from our laboratory as well as when we expected to see significant structural damage in each tissue. Due to the acute injury of the tendon, we expected to observe damage to this tissue soon after injury and chose 1 week to capture effects of acute inflammation[30]. For muscle, we have previously shown significant fibrous tissue infiltration (indicative of muscle degeneration) 3 weeks following

tendon injury[28]. In our previous studies with tendon overuse injuries[20], we have observed concomitant humeral head cartilage damage by 12 weeks after tendon injury onset.

Histology

Following tissue isolation, supraspinatus muscles and tendons (N=3) were fixed with 4% paraformaldehyde, embedded in optimum cutting temperature (OCT), and frozen in a liquid nitrogen-cooled ethanol. Supraspinatus muscle tissue was cross-sectioned and supraspinatus tendon tissue was sectioned longitudinally in 7 μm slices using a cryostat (CryoStar NX70, Thermo Fisher). Supraspinatus muscle sections were stained with Masson's trichrome and hematoxylin and eosin (H&E) stains (VWR and Richard Allan Scientific respectively). Supraspinatus tendon sections were stained with H&E and both tissues were imaged using light microscopy (Nikon TE2000). For analysis, eight sections of supraspinatus tendon (each section was imaged at both proximal and distal ends) per sample and 12 sections of supraspinatus muscle per sample were used.

Quantification of Collagen Alignment in Tendon

Tendon sections (N=3) were imaged using a Zeiss 710 NLO inverted confocal microscope (Carl Zeiss Microscopy) with a mode-locked Ti:Sapphire Chameleon Ultra laser (Coherent Inc.) in combination with non-descanned detection (NDD) to visualize the collagen fibers and quantify their orientation and distribution as previously described[31]. The laser was set to 800 nm and emission was filtered from 380 - 430 nm. Second harmonic generation (SHG) images were collected using a Plan-Apochromat 20x objective and Zeiss ZEN software. The fiber direction was estimated using OrientationJ distribution, an ImageJ plug-in (NIH) developed for directional analysis. A distribution of local angles was generated for each optical slice, where 0° aligned to the horizontal axis (length-wise along the tendon) and ± 90° to the vertical axis. The mean and standard deviation of collagen fiber orientation was calculated from the distribution of each image. For analysis, eight sections of supraspinatus tendon (each section was imaged at both proximal and distal ends) were used.

Micro-computed Tomography (μCT)

Humeral head samples (N=8) were analyzed by EPIC-μCT (Equilibrium Partitioning of an Ionic Contrast-Microcomputed tomography) based on established techniques[20,32]. EPIC-μCT involves the use of a contrast agent to better visualize less radio-opaque tissues, such as cartilage. In this work, Hexabrix (Covidien) was employed, which is negatively charged and is therefore electrostatically repulsed due to the high amounts of negative charge on biomolecules such as proteoglycans found in cartilage. Therefore, cartilage attenuation is inversely related to proteoglycan content within the tissue.

Following isolation at 1 and 12 weeks following injury, humeral heads were submerged in a 10% Hexabrix solution at 37°C for 30 min. Humeral heads were scanned in the sagittal plane with the μCT50 (Scanco Medical) at 45 kVp, 200 μA, and a 600 ms integration time. Following segmentation and reconstruction, control and injured humeral heads were evaluated for cartilage volume, cartilage thickness, and cartilage attenuation using Scanco evaluation software. Hexabrix was removed from humeral head sample by incubating in PBS at 37°C for 30 min. The same contrast-enhanced scans were used to analyze

subchondral and trabecular bone via Scanco evaluation software. Analysis of subchondral bone included thickness, volume, and density, while trabecular bone included volume and density. Additionally, the same scans were used to evaluate the subchondral bone directly under focal defects at 12 weeks. Control humeral heads were evaluated in the same region of the humeral head with equivalent numbers of slices.

Multiplex Gelatin Zymography

Following sacrifice, joint tissues were collected. Supraspinatus tendon and muscle were isolated together and then separated through fine-dissection under a stereomicroscope (Leica model: 165FC). Cartilage was carved from the humeral head using a scalpel. Tissues were homogenized using a sample grinding kit (GE Healthcare Life Sciences) and zymography lysis buffer (consists of 20 mM Tris-HCl, 5 mM EGTA, 150 mM NaCl, 20 mM glycerol-phosphate, 10 mM NaF, 1 mM sodium orthovanadate, 1% Triton-X 100, and 0.1% Tween 20 in 500 mL deionized water) with 0.1 mM freshly added leupeptin to stabilize proteins. Protein concentration was determined by microBCA kit (Thermo Fisher).

Cathepsin and MMP zymography was performed as previously described[13,33]. For supraspinatus muscle and tendon tissues (N=6-8), 15 μg of protein under non-reduced conditions were loaded on either 12.5% (cathepsin) or 10% (MMP) SDS–polyacrylamide gels laden with 0.2% gelatin substrate. For cartilage tissues (N=3-6), 10 μg of protein under non-reducing conditions were loaded onto 7.5% SDS–polyacrylamide gels laden with 0.2% gelatin substrate into both cathepsin and MMP gels. Recombinant proteins were used as positive controls on all gels. Recombinant cathepsin K (Enzo) was used for cathepsin zymograms at pH=6, recombinant cathepsin L (R&D Systems) was used for cathepsin zymograms at pH=4, and recombinant MMP-2 (R&D Systems) was used for MMP zymograms.

After separation by size, gels were washed in their respective renaturing buffer to allow proteases to return to active confirmation. Gels were incubated in their respective assay buffer at 37°C for 18 hours to allow degradation of gelatin within gels. After rinsing with DI water, gels were stained with Coomassie Brilliant Blue (Thermo Fisher) for 1 hour at room temperature and constant agitation and destained for 1 hour under the same conditions. Gels were imaged using ImageQuant LAS 4000 (GE Healthcare) and densitometry analysis was performed using ImageJ (NIH).

Immunostaining

Immunostaining of supraspinatus tendon 1 week following injury (N=3) was used to confirm the presence of inflammatory cells within the joint. Supraspinatus tendon sections were rinsed with PBS to remove OCT and blocked with 5% goat serum (R&D) for 1 hour at room temperature. Ly6g+ FITC primary antibody (abcam ab25024) diluted in 5% goat serum (1:100) was applied to sections for 1 hour at room temperature in the dark. CD68+ primary antibody (abcam ab955) was applied to sections (1:200) and incubated overnight at 4°C in a humid chamber. Following three PBS washes, secondary antibody (abcam ab150113) was added to sections (1:500) for 1 hour at room temperature in the dark. Following antibody incubation, sections were washed with PBS and incubated with Hoechst (1:1,000)

counterstain (Sigma-Aldrich) for ten minutes at room temperature in the dark. Following three PBS washes, sections were mounted and imaged immediately using confocal microscopy (Zeiss). Incubation with secondary antibody alone (i.e. no primary antibody) was used as a negative control to verify the absence of non-specific binding. To quantify the number of inflammatory cells within the tendon, ImageJ (NIH) was used to count total Hoechst stained cells and CD68+ or Ly6g+ cells using the color threshold analysis tool. Data is presented as total number of immune cells divided by total cells. The same parameters were used for injured and control images. Eight sections of supraspinatus tendon per sample were stained and quantified.

Statistical Analysis

Power analysis (G*Power software) was performed on prior data[19,20] for both zymography ($\alpha = 0.05$, $\beta = 0.8$, $\Delta = 0.48$) and μCT ($\alpha = 0.05$, $\beta = 0.8$, $\Delta = 0.75$) to determine number of animals required for this study. Prior to statistical analysis, we performed a Shapiro-Wilk normality test to ensure our data was normally distributed and could undergo parametric tests. For humeral head evaluation (bone and cartilage) via μCT and zymography analysis with multiple time points, statistical significance was determined using a two-way ANOVA and Tukey's post-hoc test ($p \leq 0.05$) in GraphPad on raw values. Densitometry analyses of zymograms are graphed as fold change compared to uninjured contralateral control samples. For humeral head evaluation of bone at a single time point, a student t-test (two-tailed, $p \leq 0.05$) was used. To determine collagen alignment within supraspinatus tendon tissue for different samples, a student's t-test ($p \leq 0.05$) was used to compare the distribution of fiber orientation from zero degrees.

RESULTS

Histology

H&E staining revealed that the control supraspinatus tendon showed dense, aligned collagen fibers and elongated cells at both the proximal and distal sections of the tendon 1 week following injury. In contrast, the injured supraspinatus tendon demonstrated cellular infiltration and changes in collagen alignment and orientation at both the proximal and distal portions of the tendon (Fig. 1a). The average alignment of collagen fibers in the control supraspinatus tendon relative to 0° was 8.5° ± 16.7° (distal) and 9.9° ± 16.0° (proximal), while the injured tendon had an average collagen alignment of −11.8° ± 51.7° (distal) and −8.3° ± 46.9° (proximal). The control supraspinatus tendon had significantly more aligned collagen fibers compared to the injured supraspinatus tendon at 1 week following injury (Fig. 1b). Supraspinatus muscle samples were qualitatively analyzed using both H&E and Masson's trichrome. Both stains revealed similar morphology in control and injury muscle fibers, with little evidence of fibrous degeneration at this time point (Fig. 2).

EPIC-μCT Analysis of Humeral Articular Cartilage, Subchondral Bone, and Trabecular Bone

Some animals developed localized loss of cartilage (focal defects) by 12 weeks following rotator cuff injury (4 of 8 animals), while no focal defects were observed in control cartilage or injured cartilage at 1 week (Fig. 3a). Focal defects had an average volume of 0.12 ± 0.09

mm^3 and did not manifest in similar regions of the humeral head cartilage between animals (Fig. S-1). Previous work investigating rat knee cartilage demonstrated consistent defects in the medial third of cartilage in an animal model of osteoarthritis[32]. Despite the presence of focal defects in half of injured animals, there were no significant differences in cartilage volume, thickness, or attenuation (inversely related to (GAG) content) between control and injury groups at either time point (Fig. 3b). Analysis of humeral head subchondral bone showed no significant differences in bone volume, thickness, or density between injured and uninjured groups at either time point (Fig. S-2a–c). However, within each group, there was a significant increase in subchondral bone volume, thickness, and density, between 1 and 12 weeks. Analysis of trabecular bone at 12 weeks showed no significant differences in bone volume between injury and control groups (Fig. S-2d–e). Analysis of subchondral bone directly under the focal defect showed no difference in thickness, but significantly greater bone density (Fig. S-2f–g) on the injured side compared to control at 12 weeks.

Active Cathepsins and MMPs in Supraspinatus Tendon

Active cathepsin L was found in pH4 and pH6 cathepsin zymograms between 37 and 25 kDa (Fig. 4a and 4c) and pro- and mature MMP-2 were detected in MMP zymograms (Fig. 4e) between 50 and 75 kDa at all three time points (1, 3, and 12 weeks post-injury). Densitometric analysis revealed significantly higher amounts of active cathepsin L in injured supraspinatus tendon with an average of 5 fold increase over control supraspinatus tendon at 1 week post-injury (Fig. 4b and 4d). Additionally, active MMP-2 was significantly increased in injured supraspinatus tendon with an average of 10 fold increase over control supraspinatus tendon at 1 and 3 weeks post-injury (Fig. 4f). There were no significant changes in protease activity at 12 weeks compared to control. Additionally, we investigated the amount of active protease over time within control supraspinatus tendon (Fig. S-3a–c). We found that there is a significant increase in the amount of active cathepsin L from 1 week to 3 weeks with a plateau between 3 and 12 weeks, whereby the amount of active cathepsin L is maintained.

Active Cathepsins and MMPs in Supraspinatus Muscle

Active cathepsin L was found in pH4 and pH6 cathepsin zymograms between 37 and 25 kDa (Fig. 5a and 5c) and pro- and mature MMP-2 were detected in MMP zymograms (Fig. 5e) between 50 and 75 kDa at all three time points (1, 3, and 12 weeks post-injury). Densitometric analysis of cathepsin pH6 and cathepsin pH4 zymograms revealed significantly higher active cathepsin L (~5 fold increase) in injured supraspinatus muscle compared to control supraspinatus muscle at 1 week post-injury (Fig. 5b and 5d). Additionally, cathepsin pH6 zymograms showed a continued increase in active cathepsin L (~5 fold increase) 3 weeks after injury (Fig. 5d). The amount of active cathepsins within the supraspinatus muscle was comparable to the uninjured control at 12 weeks following injury. Active MMP-2 was significantly increased in injured supraspinatus muscle with an average 4 fold increase over control supraspinatus muscle at 3 weeks post-injury (Fig. 5f), while there were no significant changes in the amount of active MMP at 1 and 12 weeks compared to control.

Additionally, we investigated the amount of active protease over time within control supraspinatus muscle (Fig. S-3d–f). Cathepsin pH4 zymograms demonstrated a significant increase in the amount of active cathepsin L from 1 week to 3 weeks with a plateau between 3 and 12 weeks, whereby the amount of active cathepsin L is maintained (Fig. S-3d). Conversely, cathepsin pH6 zymograms demonstrated low levels of cathepsin L with a significant increase in the amount of active cathepsin L at 12 weeks compared to 1 and 3 weeks (Fig. S-3e).

Active Cathepsins and MMPs in Humeral Head Cartilage

Following injury, active cathepsin L was found in pH4 cathepsin zymograms between 25 and 37 kDa (Fig. 6a) at all three time points (1, 3, and 12 weeks), while active cathepsin K was found in pH6 cathepsin zymograms around 75 kDa (Fig. 6c) at 1 week in cartilage (no cathepsin K was found at 3 or 12 week time points). Densitometric analysis revealed significantly higher active cathepsin L (3 fold difference) and active cathepsin K (6 fold difference) at 1 week following injury compared to control (Fig. 6b and 6d). Active MMP-2 and MMP-9 were found at all three time points (1, 3, and 12 weeks) following injury at 50 to 75 kDa and 75 to 100 kDa respectively (Fig. 6e). However, we detected no significant differences in the amount of active MMPs (Fig. 6f and 6g). Due to limited sample availability and small sample size, we were unable to perform statistical analysis on 12 week cartilage samples. Bands with a molecular weight higher than 75 kDa were not analyzed due to the inability to correctly identify the protease associated with these bands. Additionally, we investigated the level of active proteases over time within humeral head cartilage (Fig. S-3g–j) and found no significant differences between 1 and 3 weeks for cathepsins or MMPs. Due to the small sample size for 12 week cartilage, we were unable to draw statistical comparisons with previous time points.

Immunostaining for inflammatory cells

Staining for CD68+ and Ly6g+ cells indicated that both macrophages and neutrophils were present within supraspinatus tendon 1 week following injury. We found the average percentage of CD68+ cells were 24.1 ± 9.1% of all cells, while Ly6g+ cells were 31.0 ± 17.3% of all cells in injured supraspinatus tendon. Dissimilarly, control supraspinatus tendon had no CD68+ or Ly6g+ cells. Both inflammatory cell types were seen within the proximal and distal regions of the supraspinatus tendon. Moreover, we found significantly more total cells within injured supraspinatus tendon with an average of 198 ± 54 cells per region of interest, while control supraspinatus tendon had an average of 103 ± 15 cells per region of interest.

DISCUSSION

This work employed an established animal model to replicate damage that has been observed in tendon, muscle, and humeral head cartilage following acute, full-thickness rotator cuff tear in humans[5,15,18,21,23]. As demonstrated in Fig. 1, changes were observed in supraspinatus tendon morphology as early as 1 week, which was expected due to the transection of both the supraspinatus and infraspinatus tendons. Conversely, the supraspinatus muscle, which is not directly injured in this model, but suffers from secondary

effects, such as lack of neural stimulation and mechanical loading, appeared comparable to control supraspinatus muscle at 1 week (Fig. 2). However, our laboratory has previously shown significant fibrous infiltration of the supraspinatus muscle in this animal model at 3 weeks post-injury[28] and maintenance of similar levels of fibrous tissue up to 6 weeks, which aligns with other groups using similar animal models of rotator cuff injuries[27,29].

Using contrast-enhanced EPIC–uCT, we were unable to detect any differences in cartilage volume, thickness, or attenuation 12 weeks following injury (Fig. 3b). Prior work investigating denervation and tendon transection separately in a rat model has shown loss of safranin O staining in humeral head cartilage at 12 weeks[4], which should correspond to an increase in cartilage attenuation via EPIC-μCT[34,35]. However, because these results were found in a different injury model and employed a different technique, a direct comparison is limited. Additionally, we showed the presence of cartilage erosion (focal defects) within humeral head cartilage in half of all injured animals by 12 weeks. The lack of statistical difference in cartilage volume despite the presence of focal defects could be due to the fact that only half of the animals developed them, thus we would need a much larger sample size to demonstrate differences. Alternatively, it is possible the volume of cartilage lost as a focal defect was not large enough to render the overall volumes different between groups. Previous work examining humeral head cartilage following rotator cuff injury has demonstrated increased surface roughness and loss of tidemark integrity of humeral head cartilage 12 weeks post-injury in rats[4], but no indication of cartilage loss or erosion. However, contrast-enhanced μCT allows analysis of the entire humeral head and is a powerful tool to detect small defects in cartilage (Fig. S-1) that may be difficult to visualize through histological analysis[36]. A strong relationship between rotator cuff tear and subsequent degeneration of humeral head and glenoid cartilage has been seen in humans[5,37], suggesting that this animal model at least partially recapitulates this aspect of human pathology.

Further μCT analysis revealed no differences in subchondral bone thickness, volume, or density as well as no differences in trabecular bone volume or density between control and injury groups at either time point. However, we found a significant increase in subchondral bone volume, thickness, and density between 1 and 12 weeks regardless of injury (Fig. S-2a–c). This is likely due to animal growth over time. Thus, it is possible that changes to subchondral bone properties caused by the injury were concealed by this normal growth. Nevertheless, we detected subchondral bone density increased directly beneath the focal defects 12 weeks following injury (Fig. S-2). Other studies have demonstrated overall bone loss in the humeral head of rats 12 weeks following transection of the supraspinatus and infraspinatus tendons followed by tendon reattachment[38]. These differences could be the result of differences in tendon injury vs. injury + repair models. Current methods for tendon reattachment in rodents, whereby a hole is drilled through the humeral head to allow suturing of the tendon, will intrinsically create bone loss. Previous findings show a correlation between chronic rotator cuff injuries presenting with cartilage loss and decreased bone density in humans[5], suggesting that this model does not fully recapitulate aspects of bone pathology at the time points studied. However, significantly denser subchondral bone directly under the focal cartilage defects was detected in our model. This aligns with previous literature investigating instances of osteoarthritis in the knee of humans in which an

increase in bone mineral density is considered an early sign of osteoarthritis[39,40]. Combined with the presence of focal defects at 12 weeks, this model does appear to partially replicate the increased risk of developing osteoarthritis following rotator cuff tear seen in humans[5].

Examining zymography results in each tissue, overall temporal protease activity profiles were different between cathepsins and MMP-2. Specifically, cathepsins were more active in the first week, while MMP-2 maintained prolonged activity in the supraspinatus tendon between 1 and 3 weeks and increased only at 3 weeks in supraspinatus muscle. These findings align with previous work showing cathepsins can activate MMPs[26] and could also indicate the possibility of cathepsins and MMP-2 sequentially acting on collagen to increase degradation[17]. Cathepsin L, present in both supraspinatus tendon and muscle in this work, is associated with protein turnover and tissue remodeling[41]. Cathepsin L has been shown to have the ability to cleave collagen I within the telopeptide region, which is involved in intra- and intermolecular bonds between collagen units[17]. Cathepsin L activity prior to MMP-2 activity would leave MMP-2 to cleave shorter collagen I molecules and enhance overall tissue degeneration. Similarly in cartilage, where no significant MMP-2 was detected, cathepsin K, which is typically associated with bone remodeling[42], has the ability to cleave type I collagen in its native triple helix at multiple locations[17], which would allow for significant degradation without the aid of MMP-2. Thus, the type of protease and the order of appearance could have a large effect on the degree of degeneration observed in each tissue.

As a part of this study, we also investigated basal levels of active proteases change over time in each tissue. Cathepsin pH4 zymograms of supraspinatus tendon and muscle, showed a significant increase in active cathepsin L from 1 week to 3 weeks with no significant differences between 3 and 12 weeks, suggesting a plateau of active protease amounts after 3 weeks. In contrast, we did not observe any significant changes in the amounts of active MMP-2 over time in either of these tissues (Fig. S-3a–f), and no differences in active proteases over time in cartilage (Fig. S-3g–j). These findings are generally consistent with previous studies showing increased cathepsin activity in aged animals[43]. However, it should be noted that, in this work, we normalized the amount of active protease in the injured tissue to the uninjured contralateral control at each time point, therefore removing the confounding factor of age and time from the main comparisons in this work, which examined effect of injury.

In the supraspinatus muscle, significant upregulation of cathepsin L (associated with muscle atrophy in rats[18]) is observed at 1 week before obvious muscle fibrosis/atrophy could be observed at 3 weeks[28] (Fig. 5). Furthermore in Fig. 6, we see significant upregulation of active cathepsin K in cartilage at 1 week prior to visible damage at later time points (12 weeks). Thus, the onset of protease activity upregulation may not necessarily correlate with visible signs of damage. Previous findings have linked overactive proteases to degenerative damage because they were found simultaneously. For example, MMP-2 and -9 upregulation was detected in the presence of increasing muscle atrophy in rats[18,25]. Additionally, it was confirmed that cathepsin K concentration correlated to osteoarthritic severity in the knees of mice[16]. However, this work shows that proteases may be upregulated before the development of visible tissue damage and could be used as a potential biomarker to indicate

risk for downstream damage. Additionally, this suggests that protease upregulation, while brief, may have lasting effects on joint tissue and provides targets for early treatment to reduce tissue damage after traumatic injury to the shoulder.

By examining the temporal expression of proteases in multiple joint tissues simultaneously, this work begins to explore the biochemical relationship between acute damage to one tissue and eventual degradation of surrounding tissues. However, the cellular source of proteases have yet to be fully identified and are likely a combination of several tissue-resident cells, as well as cells recruited due to injury, as proteases released in one area can diffuse throughout the joint. Resident cells of the joint tissues, including tendon, muscle, cartilage, and synovium have all shown to be capable of producing proteases[8,16,18,44,45]. In addition to joint tissue cells, recruited inflammatory cells, such as macrophages and neutrophils, have the capacity to release proteases[46,47]. We have verified the presence of macrophages and neutrophils in the injured supraspinatus tendon in this animal model after 1 week (Fig. 7) and have found increased levels of myloid cells, particularly macrophages, in the supraspinatus muscle at 1 week after acute tendon injury in previous work[28]. Further investigation of the cellular source of these enzymes would help better understand the causes of the varied protease profiles observed in this work.

Regardless, protease activity returned to baseline by 12 weeks following injury in both the supraspinatus tendon and supraspinatus muscle. This observation could be due to a general resolution of the acute inflammatory response over this time period. Prior work has shown inflammatory resolution is complete by 21 days following blunt dissection of Achilles tendon in rabbits[30]. In addition, this phenomenon could be caused, in part, by biological protease regulation, whereby proteases can both activate[48] and cannibalize one another[49]. We have previously demonstrated cathepsin S has the ability to de-activate cathepsin K when present simultaneously[49]. Protease return to basal levels by 12 weeks also suggests their upregulation is a transient response to injury and that there may be a limited time window to prevent tissue degeneration through protease inhibition.

Inherent limitations of this study include the animal model chosen. Humans and rats have similar shoulder anatomies, but rats are quadruped animals and thus do not experience mechanical loading in the same way[50]. Additionally, while chosen due to the fact that this animal model developed shoulder joint damage similar to that seen in humans[5,15,18,21,23], this is an acute injury, which is not identical to how damage develops in humans in the clinical setting. A sham surgery control would have allowed the ability to distinguish how the surgery itself, which includes splitting the deltoid muscle to visualize the rotator cuff, can contribute to joint tissue degeneration. We did not investigate protease activity within the synovium or the presence of protease inhibitors over time following injury, although current findings indicate that this would be an interesting future study. Lastly, this study did not directly determine the biological cause of the visible tissue damage seen in the animal model of acute rotator cuff tear.

In summary, this work demonstrates that tissue degeneration occurs in supraspinatus tendon, supraspinatus muscle and humeral head cartilage after transection of the supra- and infraspinatus tendons in a rat model of full-thickness rotator cuff tear, and that there is

significant protease upregulation in all three tissues, each with different temporal profiles. Interestingly, increased protease activity was found at early time points in all tissues tested, even though only the tendon was injured directly. Both cathepsin L and MMP-2 activity were upregulated in supraspinatus tendon at 1 week in Fig. 4, which coincided with visible damage. Conversely, supraspinatus muscle tissue experienced upregulated cathepsin L activity at 1 week with no obvious structural damage at this time point in Fig. 5. Active cathepsin K and L were upregulated in cartilage 1 week after injury (Fig. 6), and subsequent damage in the form of focal defects at 12 weeks following injury was found in ~half of all animals (Fig. 3). A more comprehensive understanding of biochemical changes to joint tissue over time following rotator cuff tear will better inform ideal intervention times and treatments for each tissue. These results demonstrate concomitant degeneration in a number of rotator cuff tissues after traumatic injury and suggest that early intervention addressing multiple tissues simultaneously may be required to prevent joint degeneration after rotator cuff tear.

Supplementary Material

Refer to Web version on PubMed Central for supplementary material.

ACKNOWLEDGEMENTS

The authors would like to thank Akia Parks for her help with gelatin zymography, Angela Lin for her assistance in performing μCT scans and analysis, and Dr. Wei Sun and Fatiesa Sulejmani for their assistance in generating and analyzing SHG images of tendon collagen. The authors would also like to thank Liane Tellier and Alexandra Brimeyer for their help completing surgeries. This content is solely the responsibility of the authors and does not necessarily represent the official views of the National Institutes of Health.

REFERENCES

1. Ricchetti ET, Aurora A, Iannotti JP, Derwin KA. Scaffold devices for rotator cuff repair. J Shoulder Elb Surg. 2012;21(2):251–265.
2. Yadav H, Nho S, Romeo A, MacGillivray JD. Rotator cuff tears: Pathology and repair. Knee Surgery, Sport Traumatol Arthrosc. 2009;17(4):409–421.
3. Goutallier D, Postel JM, Bernageau J, Lavau L VM. Fatty muscle degeneration in cuff ruptures. Pre- and postoperative evaluation by CT scan. Clin Orthop Relat Res. 1994;304:78–83.
4. Kramer EJ, Bodendorfer BM, Laron D, et al. Evaluation of cartilage degeneration in a rat model of rotator cuff tear arthropathy. J Shoulder Elb Surg. 2013;22(12):1702–1709.
5. Neer CS; Craig EV; Fukuda H. Cuff-tear arthropathy. J Bone Jt Surg. 1983;65(9):1232–1244.
6. Brew K, Nagase H. The tissue inhibitors of metalloproteinases (TIMPs): An ancient family with structural and functional diversity. Biochim Biophys Acta. 2010;1803(1):55–71. [PubMed: 20080133]
7. Maeda E, Fleischmann C, Mein CA, Shelton JC, Bader DL, Lee DA. Functional analysis of tenocytes gene expression in tendon fascicles subjected to cyclic tensile strain Functional analysis of tenocytes gene expression in tendon fascicles. Connect Tissue Res. 2010;51:434–444. [PubMed: 20497018]
8. Arnoczky SP, Lavagnino M, Egerbacher M. The mechanobiological aetiopathogenesis of tendinopathy: is it the over-stimulation or the under-stimulation of tendon cells? Int J Exp Pathol. 2007;88:217–226. [PubMed: 17696902]
9. Punturieri A, Filippov S, Allen E, et al. Regulation of Elastinolytic Cysteine Proteinase Activity in Normal and Cathepsin K–deficient Human Macrophages. J Exp Med. 2000;196(6):789–799.

10. Starkey PM, Barrett AJ, Burleigh MC. The degradation of articular collagen by neutrophil proteinases. Biochim Biophys Acta - Enzymol. 1977;483(2):386–397.
11. Thomopoulos S, Parks WC, Rifkin DB, Derwin KA. Mechanisms of tendon injury and repair. J Orthop Res. 2015;33(6):832–839. [PubMed: 25641114]
12. Huegel J, Williams AA, Soslowsky LJ. Rotator Cuff Biology and Biomechanics: a Review of Normal and Pathological Conditions. Curr Rheumatol Rep. 2015;17(1):476. [PubMed: 25475598]
13. Wilder CL, Park K-Y, Keegan PM, Platt MO, Coulter WH. Manipulating substrate and pH in zymography protocols selectively distinguishes cathepsins K, L, S, and V activity in cells and tissues. Arch Biochem Biophys. 2011;516:52–57. [PubMed: 21982919]
14. Wilder CL, Walton C, Watson V, et al. Differential cathepsin responses to inhibitor-induced feedback: E-64 and cystatin C elevate active cathepsin S and suppress active cathepsin L in breast cancer cells. Int J Biochem Cell Biol. 2016;79:198–208.
15. Kozawa E, Cheng XW, Urakawa H, et al. Increased expression and activation of cathepsin K in human osteoarthritic cartilage and synovial tissues. J Orthop Res. 2016;34(1):127–134. [PubMed: 26241216]
16. Konttinen YT, Mandelin J, Li TF, et al. Acidic cysteine endoproteinase cathepsin K in the degeneration of the superficial articular hyaline cartilage in osteoarthritis. Arthritis Rheum. 2002;46(4):953–960. [PubMed: 11953972]
17. Garnero P, Borel O, Byrjalsen I, et al. The Collagenolytic Activity of Cathepsin K Is Unique among Mammalian Proteinases. J Biol Chem. 1998;273(48):32347–32352. [PubMed: 9822715]
18. Deval C, Mordier S, Obled C, et al. Identification of cathepsin L as a differentially expressed message associated with skeletal muscle wasting. Biochem J. 2001;360:143–150. [PubMed: 11696001]
19. Seto SP, Parks AN, Qiu Y, et al. Cathepsins in Rotator Cuff Tendinopathy: Identification in Human Chronic Tears and Temporal Induction in a Rat Model. Ann Biomed Eng. 2015;43(9):2036–2046. [PubMed: 25558848]
20. Parks AN, McFaline-Figueroa J, Coogan A, et al. Supraspinatus tendon overuse results in degenerative changes to tendon insertion region and adjacent humeral cartilage in a rat model. J Orthop Res. 2016:1–9.
21. Riley GP, Curry V, Degroot J, et al. Matrix metalloproteinase activities and their relationship with collagen remodelling in tendon pathology. Matrix Biol. 2002;21:185–195. [PubMed: 11852234]
22. Yoshihara Y, Hamada K, Nakajima T, Fujikawa K, Fukuda H. Biochemical markers in the synovial fluid of glenohumeral joints from patients with rotator cuff tear. J Orthop Res Off Publ Orthop Res Soc. 2001;19(4):573–579.
23. Jackson MT, Moradi B, Smith MM, Jackson CJ, Little CB. Activation of Matrix Metalloproteinases 2, 9, and 13 by Activated Protein C in Human Osteoarthritic Cartilage Chondrocytes. Arthritis Rheumatol. 2014;66(6):1525–1536. [PubMed: 24574263]
24. Beckett J, Jin W, Schultz M, et al. Excessive running induces cartilage degeneration in knee joints and alters gait of rats. J Orthop Res. 2012;30(10):1604–1610. [PubMed: 22508407]
25. Reznick AZ, Menashe O, Bar-Shai M, Coleman R, Carmeli E. Expression of matrix metalloproteinases, inhibitor, and acid phosphatase in muscles of immobilized hindlimbs of rats. Muscle and Nerve. 2003;27(1):51–59. [PubMed: 12508295]
26. Christensen J, Shastri VP. Matrix-metalloproteinase-9 is cleaved and activated by cathepsin K. BMC Res Notes. 2015;8(1):322. [PubMed: 26219353]
27. Liu X, Laron D, Natsuhara K, et al. A mouse model of massive rotator cuff tears. J Bone Jt Surg - Ser A. 2012;94(7):e41.
28. Tellier L, Krieger J, Sellick A, et al. Localized SDF-1 Delivery Increases Pro-Healing Bone Marrow-Derived Cells in the Supraspinatus Muscle Following Severe Rotator Cuff Injury. Regen Eng Transl Med. 2018.
29. Liu X, Manzano G, Kim HT, Feeley BT. A rat model of massive rotator cuff tears. J Orthop Res. 2011;29(4):588–595. [PubMed: 20949443]
30. Enwemeka CS. Inflammation, Cellularity, and Fibrillogenesis in Regenerating Tendon: Implications for Tendon Rehabilitation. Phys Ther. 1989;69(10):816–825. [PubMed: 2780808]

31. Sulejmani F, Pokutta-Paskaleva A, Salazar O, Karimi M, Sun W. Mechanical and Structural Analysis of the Pulmonary Valve in Congenital Heart Defects: A Presentation of Two Case Studies. J Mech Behav Biomed Mater. 2018. doi:10.1016/j.jmbbm.2018.08.053.
32. Thote T, Lin ASP, Raji Y, et al. Localized 3D analysis of cartilage composition and morphology in small animal models of joint degeneration. Osteoarthr Cartil. 2013;21(8):1132–1141. [PubMed: 23747340]
33. Kupai K, Szucs G, Cseh S, et al. Matrix metalloproteinase activity assays: Importance of zymography. J Pharmacol Toxicol Methods. 2010;61(2):205–209. [PubMed: 20176119]
34. Xie L, Lin ASP, Levenston ME, Guldberg RE, Woodruff GW. Quantitative assessment of articular cartilage morphology via EPIC-μCT. Osteoarthr Cartil. 17:313–320. [PubMed: 18789727]
35. Palmer AW, Guldberg RE, Levenston ME, Woodruff GW. Analysis of cartilage matrix fixed charge density and three-dimensional morphology via contrast-enhanced microcomputed tomography. Proc Natl Acad Sci U S A. 2006;103(51):19255–19260. [PubMed: 17158799]
36. Willett NJ, Thote Z T, Hart M, et al. Quantitative pre-clinical screening of therapeutics for joint diseases using contrast enhanced micro-computed tomography. 2016.
37. Hsu HC, Luo ZP, Stone JJ, Huang TH, An KN. Correlation between rotator cuff tear and glenohumeral degeneration. Acta Orthop Scand. 2003;74(1):89–94. [PubMed: 12635800]
38. Killian ML, Cavinatto L, Shah SA, et al. The effects of chronic unloading and gap formation on tendon-to-bone healing in a rat model of massive rotator cuff tears. J Orthop Res. 2014;32(3):439–447. [PubMed: 24243733]
39. Buckland-Wright C, Sc D. Subchondral bone changes in hand and knee osteoarthritis detected by radiography. Osteoarthr Cartil. 2004;12:10–19.
40. Reece DS, Thote T, Lin ASP, Willett NJ, Guldberg RE. Contrast enhanced μCT imaging of early articular changes in a pre-clinical model of osteoarthritis. Osteoarthr Cartil. 2018;26(1):118–127. [PubMed: 29107695]
41. Maciewicz RA, Etherington DJ. A comparison of four cathepsins (B, L, N and S) with collagenolytic activity from rabbit spleen. Biochem J. 1988;256(2):433–440. [PubMed: 3223923]
42. Bose K Proteases in Apoptosis: Pathways, Protocols and Translational Advances.; 2015.
43. Keppler D, Walter R, Perez C, Sierra F. Increased expression of mature cathepsin B in aging rat liver. Cell Tissue Res. 2000;302:181–188. [PubMed: 11131129]
44. Drake FH, Dodds RA, James IE, et al. Cathepsin K, but Not Cathepsins B, L, or S, Is Abundantly Expressed in Human Osteoclasts. J Biol Chem. 1996;271(21):12511–12516. [PubMed: 8647859]
45. Hou W-S, Li W, Keyszer G, et al. Comparison of Cathepsins K and S Expression Within the Rheumatoid and Osteoarthritic Synovium. Arthritis Rheum. 2002;46(3):663–674. [PubMed: 11920402]
46. Everts V, Hou WS, Rialland X, et al. Cathepsin K Deficiency in Pycnodysostosis Results in Accumulation of Non-Digested Phagocytosed Collagen in Fibroblasts. Calcif Tissue Int. 2003;73(4):380–386. [PubMed: 12874701]
47. Novinec M, Grass RN, Stark WJ, Turk V, Baici A, Lenarčič B. Interaction between Human Cathepsins K, L, and S and Elastins Mechanism Of Elastinolysis And Inhibition By Macromolecular Inhibitors. 2007.
48. Mcqueney MS, Amegadzie BY, D ‘alessio K, et al. Autocatalytic Activation of Human Cathepsin K. J Biol Chem. 1997;272(21):13955–13960. [PubMed: 9153258]
49. Barry ZT, Platt MO. Cathepsin S Cannibalism of Cathepsin K as a Mechanism to Reduce Type I Collagen Degradation. J Biol Chem. 2012;287(33):27723–27730. [PubMed: 22730330]
50. Soslowsky L, Carpenter JE, Debano CM, Soslowsky LJ. Development and use of an animal model for investigations on rotator cuff disease.

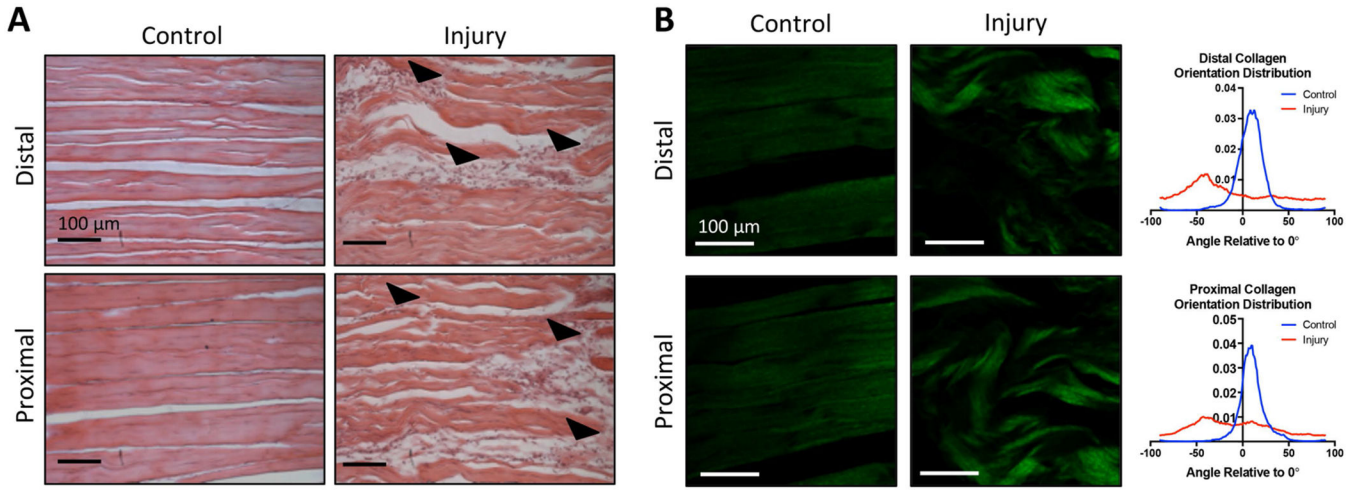

Figure 1: One week after injury tendon undergoes noticeable damage.

(A) H&E staining of longitudinally-sectioned tendon reveals damage 1 week after injury, indicated by changes in collagen structure and cellular infiltration (arrowheads) (B) Second Harmonic Generation images of collagen within tendon sections with quantification of orientation distribution. The average alignment of collagen fibers in the control supraspinatus tendon relative to 0° was 8.5° ± 16.7° (distal) and 9.9° ± 16.0° (proximal), while the injured supraspinatus tendon had an average collagen alignment of −11.8° ± 51.7° (distal) and −8.3° ± 46.9° (proximal) relative to 0°. The orientation of collagen fibers in injured supraspinatus tendon was significantly different from control ($p<0.05$). Scale bars are 100 μm.

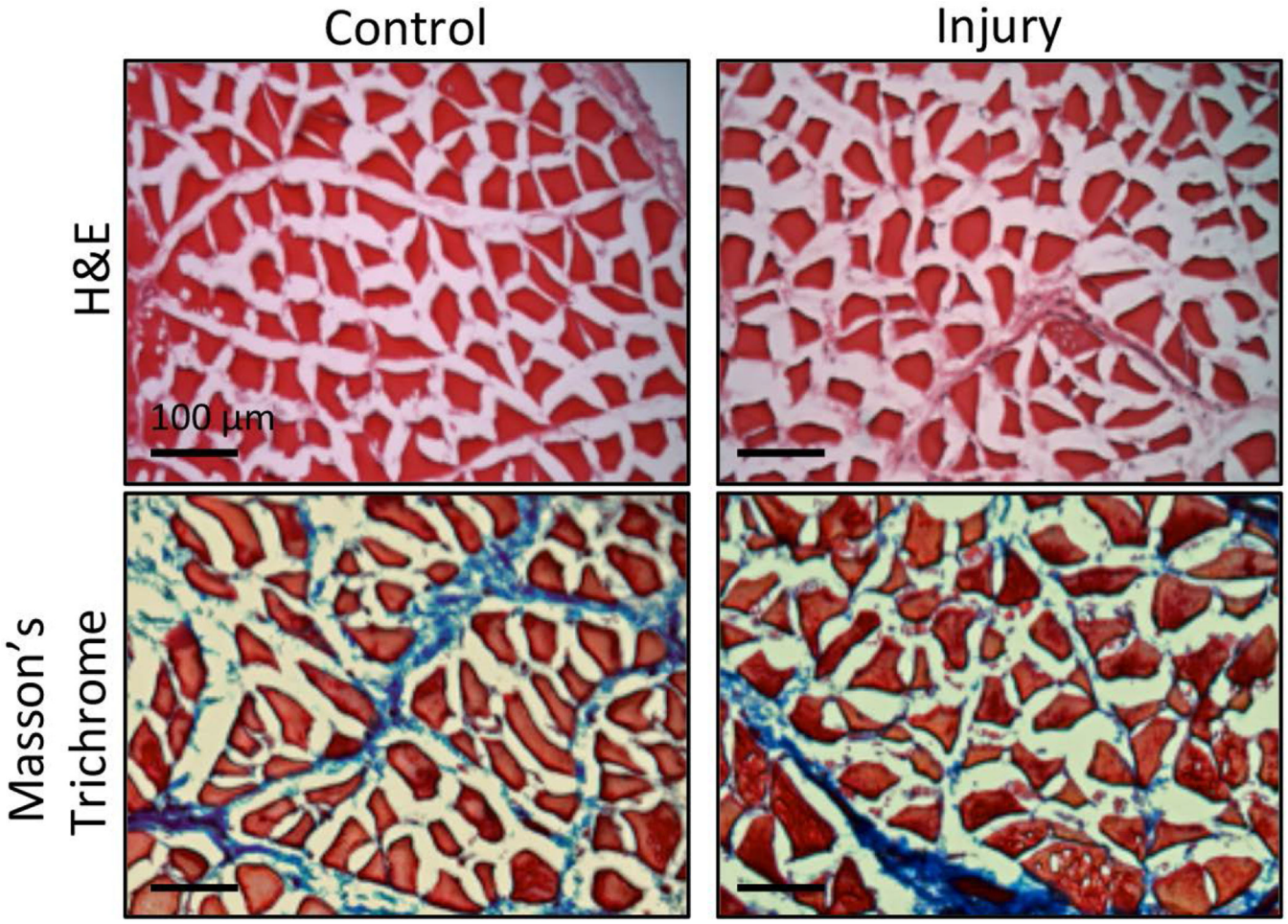

Figure 2: One week after injury muscle remains similar to control.

H&E and Masson's trichrome staining of muscle cross-sections shows no differences compared to uninjured control 1 week after injury. Scale bar is 100 μm.

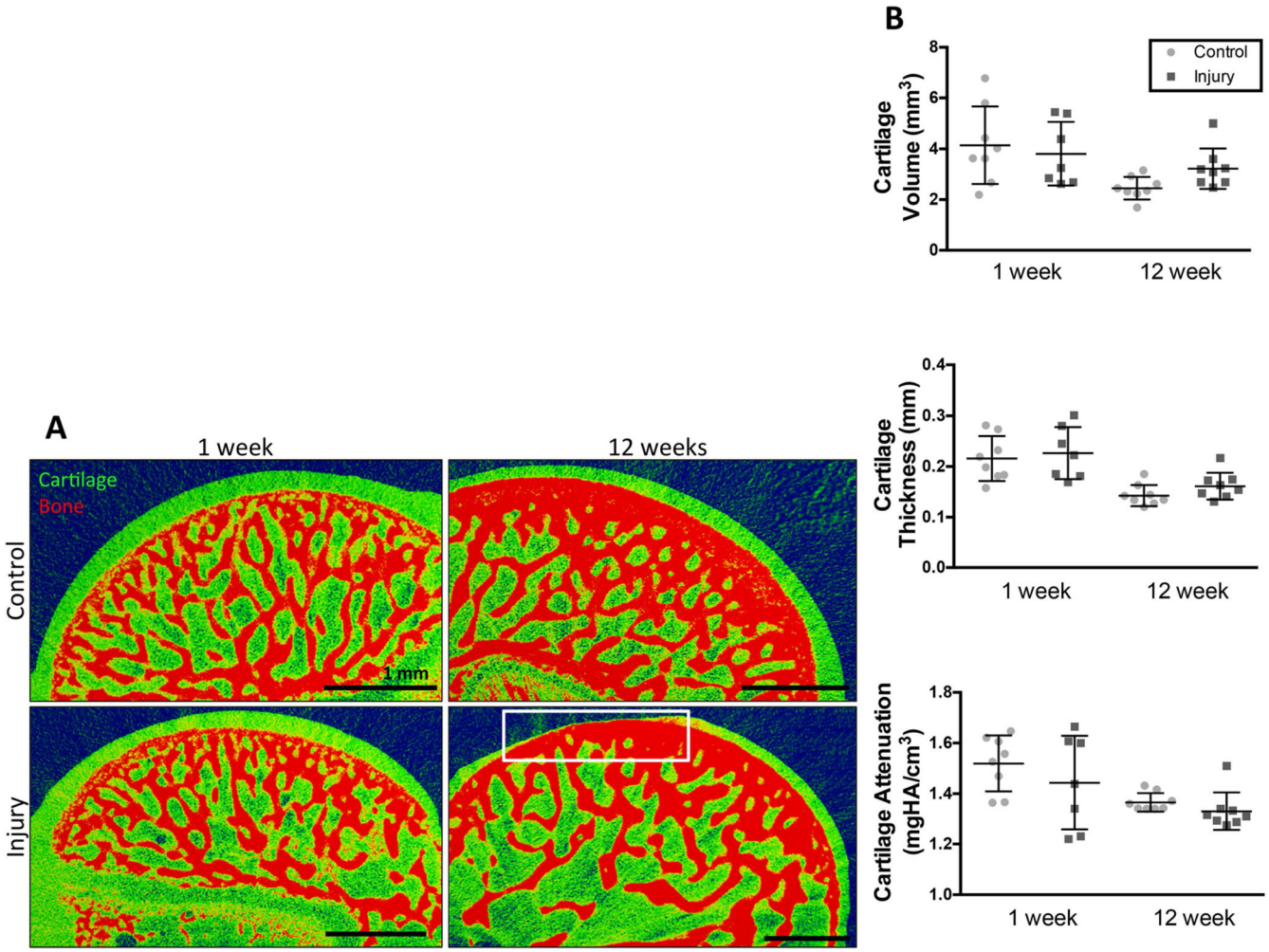

Figure 3: Contrast enhanced microCT reveals focal defects within cartilage 12 weeks post-injury.
(A) contrast enhanced microCT of humeral heads. Loss of cartilage (focal defects) highlighted in white box. Defects present in 4 out of 8 animals. N=8. scale bar = 1mm. (B) Evaluation of cartilage thickness, cartilage volume, and cartilage attenuation. N=8, no significant differences present.

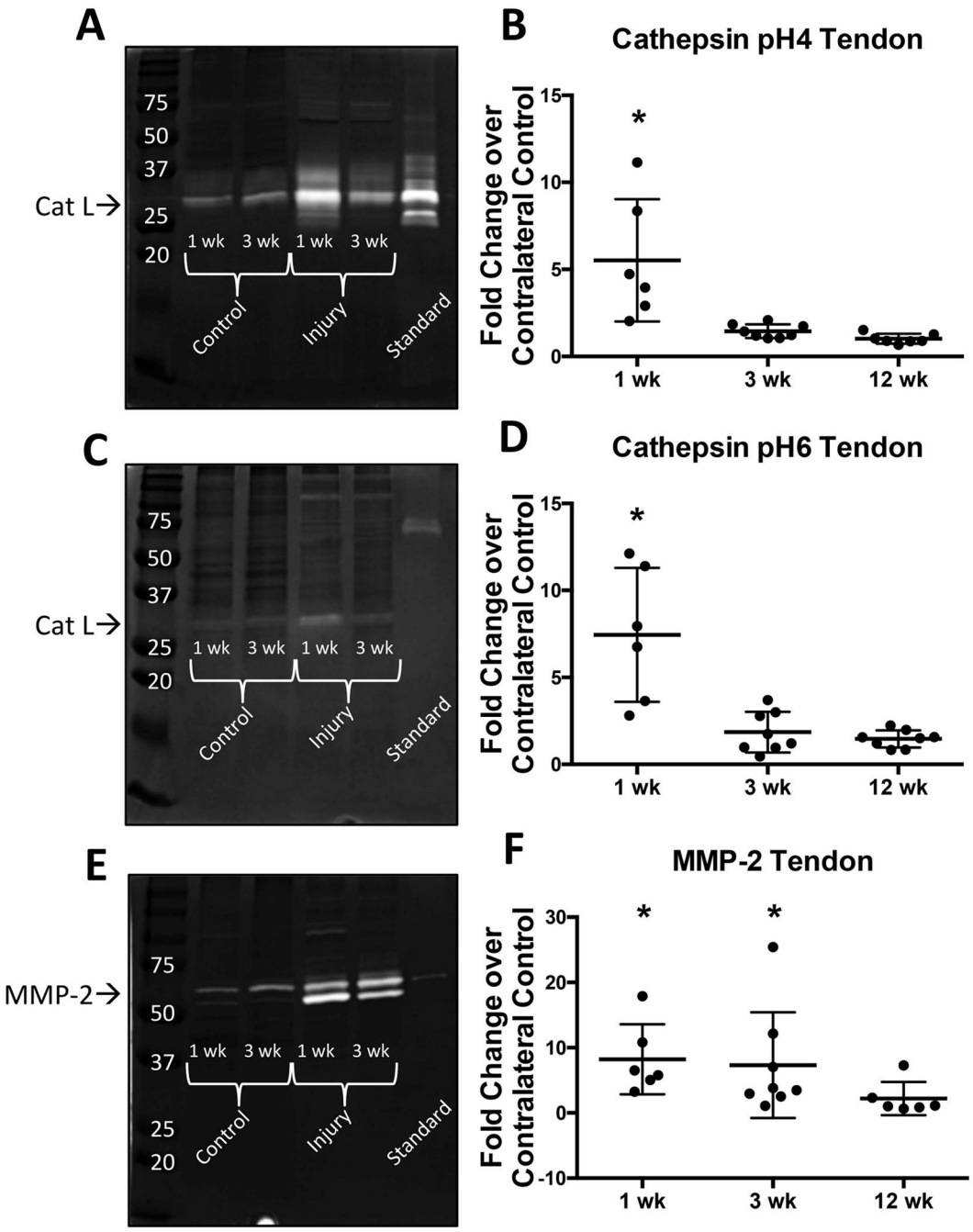

Figure 4: Gelatin zymography of tendon shows significant increase of proteases following injury.
(A-B) cathepsin (pH=4 buffer) zymography gel and densitometry quantification (C-D) cathepsin (pH=6 buffer) zymography gel and densitometry quantification (E-F) MMP zymography gel and densitometry quantification. Recombinant protein used as standard: cathepsin L, cathepsin K, MMP-2 respectively. *p<0.05. N=6-8.

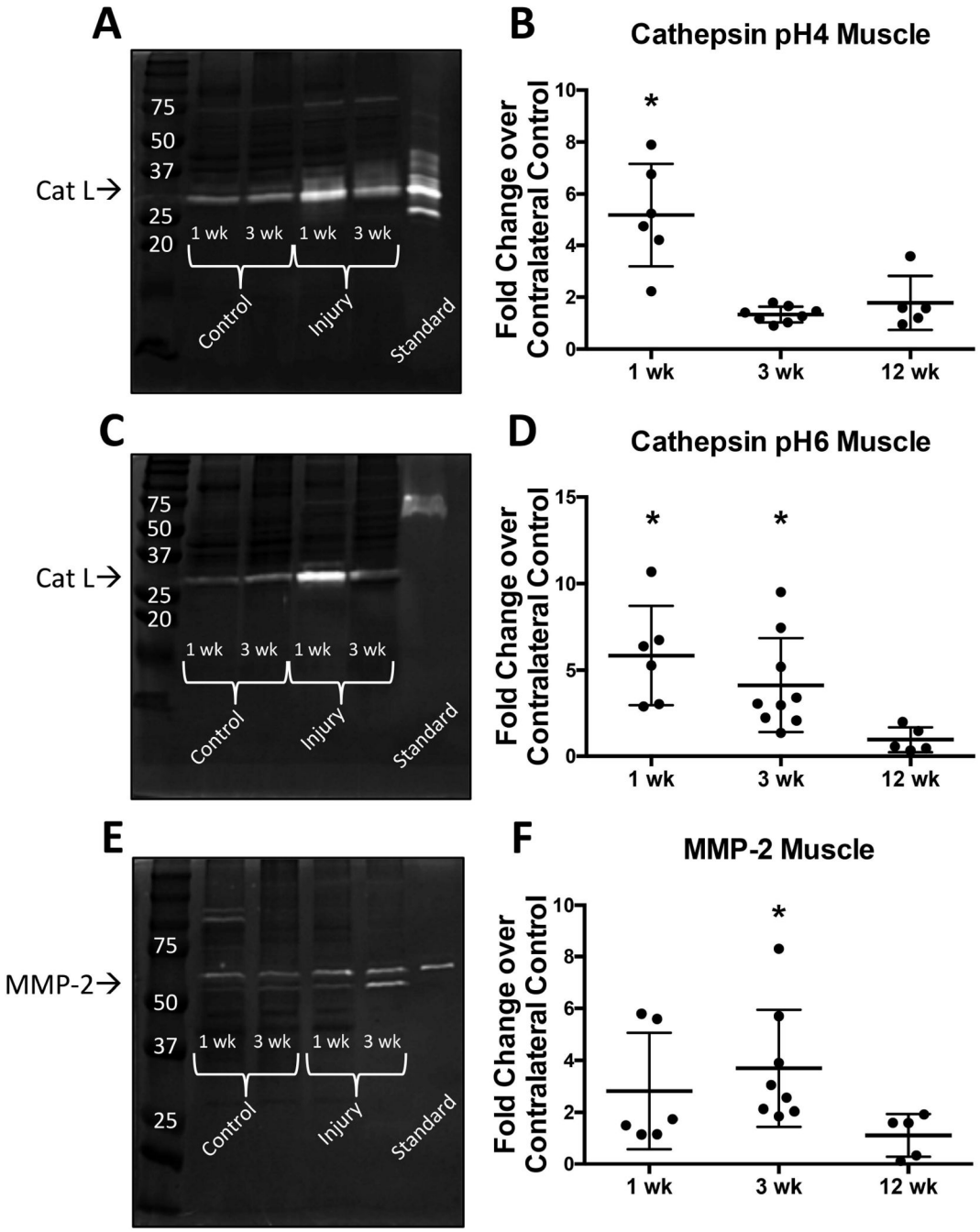

Figure 5: Gelatin zymography of muscle shows significant increase of proteases following injury.
(A-B) cathepsin (pH=4 buffer) zymography gel and densitometry quantification (C-D) cathepsin (pH=6 buffer) zymography gel and densitometry quantification (E-F) MMP zymography gel and densitometry quantification. Recombinant protein used as standard: cathepsin L, cathepsin K, MMP-2 respectively. *p<0.05. N=6-8.

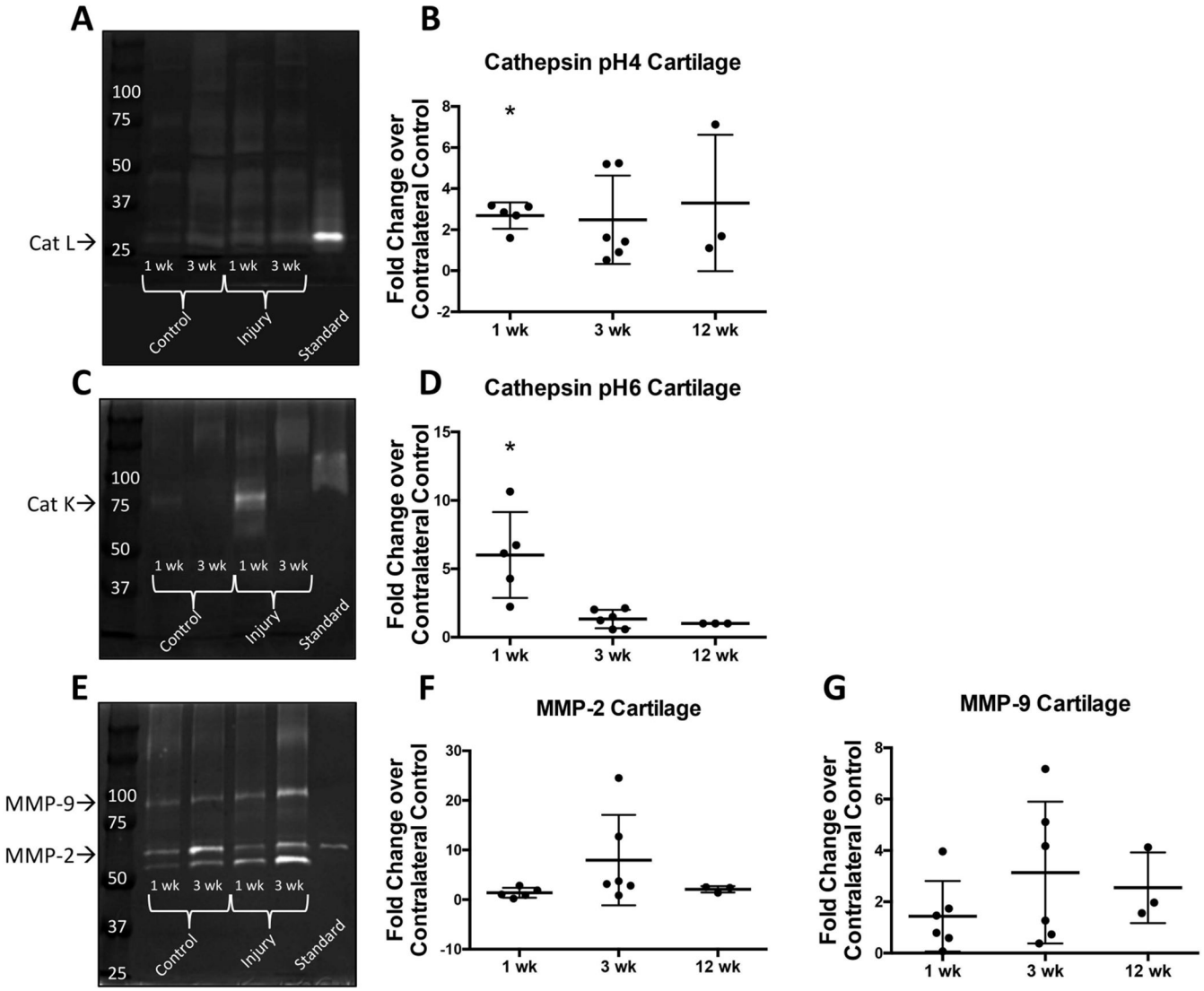

Figure 6: Gelatin zymography of cartilage shows significant increase of proteases following injury.

(A-B) cathepsin (pH=4 buffer) zymography gel and densitometry quantification (C-D) cathepsin (pH=6 buffer) zymography gel and densitometry quantification (E-G) MMP zymography gel and densitometry quantification. Recombinant protein used as standard: cathepsin L, cathepsin K, MMP-2 respectively. *$p<0.05$. N=3. 12 week cartilage samples cannot be statistically analyzed due to low sample size.

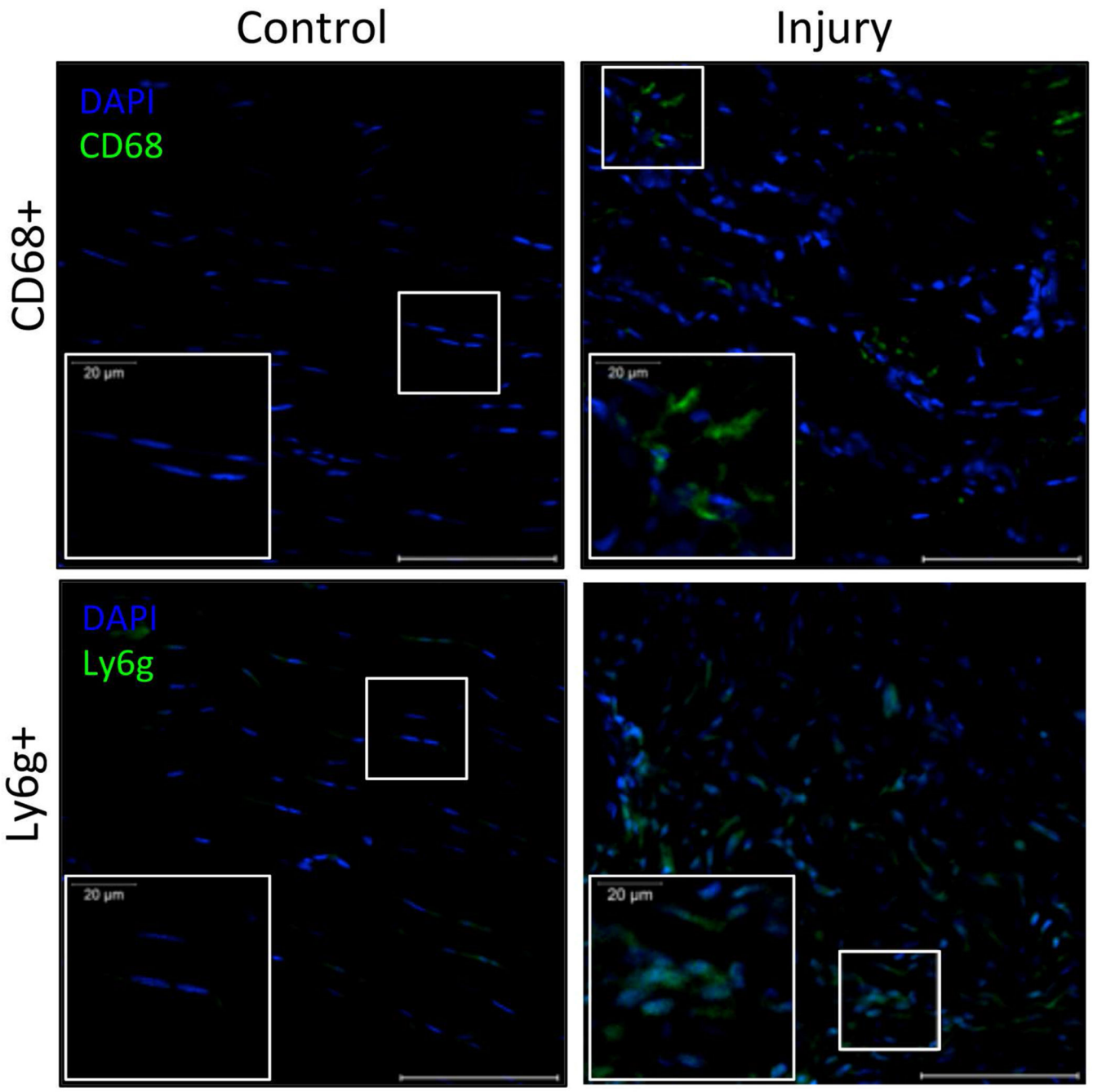

Figure 7: Immunostaining of tendon shows significantly higher prevalence of macrophage (CD68+) and neutrophil (Ly6g+) markers in injured tendon 1 week post-injury compared to uninjured control.

Quantitative analysis via color thresholding demonstrated there was significantly more CD68+ cells in injured supraspinatus tendon (24.1 ± 9.1% of all cells) compared to 0% in control tendon ($p<0.05$). Additionally, there was significantly more Ly6g+ cells in injured supraspinatus tendon (31.0 ± 17.3% of all cells) compared to 0% in control supraspinatus

tendon ($p<0.05$). DAPI used as nuclear stain. Image scale bar = 100 um, insert scale bar = 20 um.

Table 1:

Experimental design and outcome measures performed in all three joint tissues over time.

	1 week	3 weeks	12 weeks
Supraspinatus Tendon	Zymography (N=6)	Zymography (N=8)	Zymography (N=6)
	Histology (N=3)	-	-
Supraspinatus Muscle	Zymography (N=6)	Zymography (N=8)	Zymography (N=6)
	Histology (N=3)	-	-
Humeral Head Cartilage	Zymography (N=6)	Zymography (N=6)	Zymography (N=3)
	EPIC μCT (N=8)	-	EPIC μCT (N=8)